

Photolabile Protecting Groups Based on the Singlet State Photodecarboxylation of Xanthone Acetic Acid

Jessie A. Blake,[†] Matthew Lukeman,[‡] and Juan C. Scaiano^{*†}

*Department of Chemistry, University of Ottawa, Ottawa, Ontario, Canada K1N 6N5, and
Department of Chemistry, Acadia University, 6 University Avenue, Wolfville, NS, Canada, B4P 2R6*

Received December 4, 2008; E-mail: tito@photo.chem.uottawa.ca

Abstract: A new photolabile protecting group (PPG) for carboxylic acids and amines has been developed based on the rapid singlet state photodecarboxylation of xanthone acetic acids with several features that are superior to many other systems. We demonstrate that the “xanthonate” PPG can photorelease carboxylic acids and amines (via the carbamates) quantitatively in neutral phosphate buffer solution with a remarkable “uncaging cross section” ($\Phi \cdot \epsilon = 3900 \text{ M}^{-1} \text{ cm}^{-1}$ with UVA irradiation). Advantageous features include a high reaction efficiency ($\Phi > 0.6$), very clean photochemistry, subnanosecond release kinetics, good water solubility, and excellent UVA absorption. Investigations into the mechanism of release employing nanosecond laser flash photolysis (LFP), time-resolved and steady-state fluorescence spectroscopy, and product studies support an initial rapid decarboxylation from the singlet excited state to form a carbanion intermediate which undergoes a very rapid β -elimination of the carboxylate or carbamate leaving group, all occurring on the subnanosecond time scale.

Introduction

Molecules capable of releasing active groups with light activation, termed “photocages” or “photolabile protecting groups” (PPGs), are useful in a wide variety of applications when spatial and/or temporal control is desired. The most common of these is the time-resolved study of fast biological processes requiring PPGs capable of releasing signaling molecules very rapidly, with high quantum yield and clean photochemistry.¹ The application of PPGs is by no means limited to biochemical kinetic studies and also includes photolithography, DNA synthesis and microarray fabrication,² and solid state synthesis³ to name a few. Although they have not yet been used in drug delivery to our knowledge, the possibility is being explored.⁴

While a number of PPGs have been reported and studied,^{1,5} each has a particular set of limitations, often including a low quantum yield of release and/or slow release kinetics. For example, the most commonly used system, based on *o*-nitrobenzyl (*o*-NB) photochemistry, has a relatively slow release rate following light excitation, on the scale of microseconds to seconds for carboxylates⁶ and alcohols,⁷ respectively, precluding

the study of very fast processes. The *o*-NB group also suffers from poor water solubility and the formation of reactive nitrosoaldehyde byproducts, drawbacks which render these cages unappealing for many applications.^{7,8}

We have recently reported the new “ketoprofenate” PPG⁹ that offers many advantages to those currently in use, including good water solubility, fast release kinetics, and clean, efficient photochemistry. The ketoprofenate PPG takes advantage of the highly efficient ($\Phi = 0.75$)¹⁰ photodecarboxylation of ketoprofen (**1**) (Scheme 1).^{11–13}

In its carboxylate form, **1** undergoes decarboxylation upon irradiation to yield a short-lived carbanion intermediate that is detectable by nanosecond laser flash photolysis ($\lambda = 580 \text{ nm}$) and is protonated rapidly by water ($k = 4.6 \times 10^6 \text{ s}^{-1}$). The ketoprofenate PPG (**2**) is a derivative of ketoprofen that contains leaving groups positioned β to the carboxylate group (and β to the incipient carbanion). For **2a–f**, the photogenerated carbanion has an additional elimination pathway available that effectively competes with protonation by water (Scheme 2).⁹ For those derivatives possessing good leaving groups (**2a–e**), protonation by water is not observed, and only rapid elimination to release

[†] University of Ottawa.

[‡] Acadia University.

- (1) Goeldner, M.; Givens, R. *Dynamic Studies in Biology*; Wiley-VCH: Weinheim, 2005; Vol. 1.
- (2) Flickinger, S. T.; Patel, M.; Binkowski, B. F.; Lowe, A. M.; Li, M. H.; Kim, C.; Cerrina, F.; Belshaw, P. J. *Org. Lett.* **2006**, *8* (11), 2357–2360.
- (3) Kessler, M.; Glatthar, R.; Giese, B.; Bochet, C. G. *Org. Lett.* **2003**, *5* (8), 1179–1181.
- (4) Montgomery, H. J.; Perdicakis, B.; Fishlock, D.; Lajoie, G. A.; Jervis, E.; Guillemette, J. G. *Bioorg. Med. Chem.* **2002**, *10*, 1919–1927.
- (5) Pelliccioli, A. P.; Wirz, J. *Photochem. Photobiol. Sci.* **2002**, *1*, 441–458.
- (6) Wieboldt, R.; Gee, K. R.; Niu, L.; Ramesh, D.; Carpenter, B. K.; Hess, G. P. *Proc. Natl. Acad. Sci. U.S.A.* **1994**, *91*, 8752–8756.

(7) Il'ichev, Y. V.; Schworer, M. A.; Wirz, J. *J. Am. Chem. Soc.* **2004**, *126*, 4581–4595.

(8) Corrie, J. E. T.; Barth, A.; Munasinghe, V. R. N.; Trentham, D. R.; Hutter, M. C. *J. Am. Chem. Soc.* **2003**, *125*, 8546–8554.

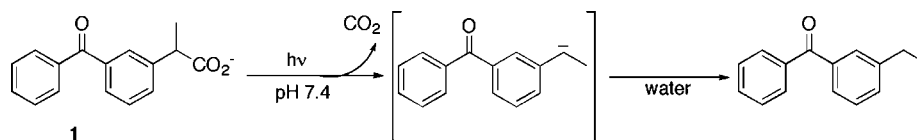
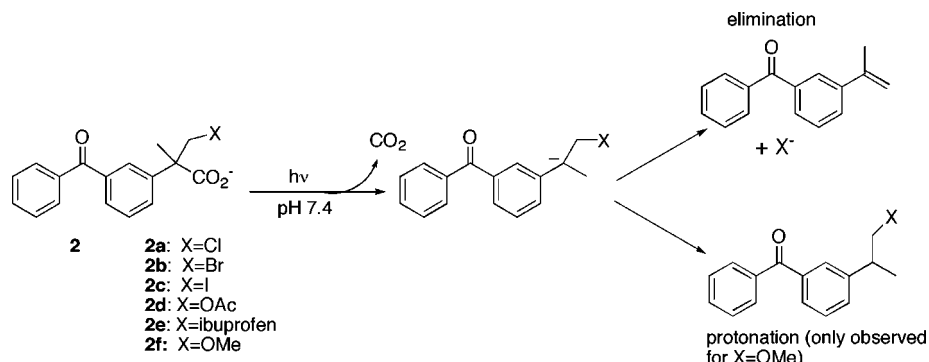
(9) Lukeman, M.; Scaiano, J. C. *J. Am. Chem. Soc.* **2005**, *127* (21), 7698–7699.

(10) Costanzo, L. L.; De Guidi, G.; Condorelli, G.; Cambria, A.; Fama, M. *Photochem. Photobiol.* **1989**, *50* (3), 359–365.

(11) Martinez, L. J.; Scaiano, J. C. *J. Am. Chem. Soc.* **1997**, *119* (45), 11066–11070. (b) Cosa, G.; Martinez, L. J.; Scaiano, J. C. *Phys. Chem. Chem. Phys.* **1999**, *1* (15), 3533–3537.

(12) Bosca, F.; Marin, F. L.; Miranda, M. A. *Photochem. Photobiol.* **2001**, *74* (5), 637–655. (a) Monti, S.; Sortino, S.; De Guidi, G.; Marconi, G. *J. Chem. Soc., Faraday Trans.* **1997**, *93* (13), 2269–2275.

(13) Cosa, G.; Llauger, L.; Scaiano, J. C.; Miranda, M. A. *Org. Lett.* **2002**, *4* (18), 3083–3085.

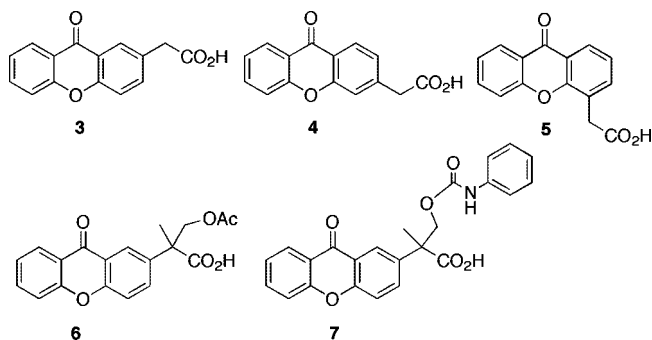
Scheme 1. Ketoprofen Photodecarboxylation and Protonation**Scheme 2.** Elimination and Protonation Pathways of Ketoprofen Derivatives

the leaving group takes place, with rate constants estimated to be greater than 10^8 s^{-1} . Submicrosecond release of a primary alcohol was also achieved using this strategy (for **2f**), although protonation by water reduced the elimination yield for this derivative.

Although the ketoprofenate PPG offers many advantages, one limitation stems from its poor absorption above 300 nm, a consideration that is particularly important for use in biological systems since wavelengths in the UVB region (280–315 nm) will cause extensive photodamage to cells. The ketoprofenate cage is based on the benzophenone chromophore whose longest absorption wavelength band at $\lambda \sim 340 \text{ nm}$ has a very low extinction coefficient because it arises from a forbidden n,π^* transition. We recognized that the structurally related xanthone chromophore has much better absorption above 300 nm and might therefore be a better choice for the design of next-generation carbanion-mediated PPGs. Xanthone has been the chromophore of choice in a limited number of new PPGs.¹⁴ While these examples share with our contribution the advantages of xanthone absorption spectroscopy, they operate via a completely different mechanism to the photorelease described here. In both previous examples xanthone is used simply as a sensitizer for electron transfer.

The development of xanthone PPGs of course is only possible if xanthone-based relatives of **1** (2-(9-oxo-9H-xanthenyl)acetic acids or xanthone acetic acids) are also able to undergo efficient photodecarboxylation to give carbanion intermediates, a reaction that was not known before we embarked on this study. We recently reported a preliminary study on the photochemistry and photophysics of three xanthone acetic acid isomers (**3–5**) at physiological pH.¹⁵ Two of these were found to photodecarboxylate with an efficiency approaching that of **1**. In an effort to capitalize on this efficient photochemistry, we also designed and prepared new “xanthone” PPGs **6** and **7** to release acetate and aniline (via its carbamate), respectively, on irradiation with UVA light in aqueous solution. Acetate and

aniline were chosen as representative examples of carboxylic acids and amines, which are functional groups commonly found in bioactive molecules. Herein we report the rapid and efficient elimination of these leaving groups from **6** and **7** upon UVA exposure in neutral aqueous solution. In addition, we elaborate on the photochemistry and photophysics of the parent molecules **3–5**.



Results and Discussion

Synthesis. Xanthone acetic acids **3–5** were initially prepared by the Ulmann coupling of *o*-iodobenzoic acid and the appropriate hydroxyphenylacetic acid, followed by acid catalyzed ring closing with an overall yield of $\sim 30\%$ according to literature procedure.¹⁶ We were able to improve the overall yield of **3** to 40% by starting with 4-hydroxyphenyl acetate ethyl ester rather than 4-hydroxyphenylacetic acid. All three xanthone acetic acids exhibit a reasonably strong absorption band near 350 nm, showing that these derivatives do indeed possess superior absorption to ketoprofen in this region (Figure 1). Derivatives **6** and **7** were both made from the common synthetic intermediate **10**, which itself was made by first methylating the benzylic carbon of **8** by treatment with LDA and CH_3I in dry THF to give **9** and finally hydroxymethylating by treatment with paraformaldehyde in DMSO containing K_2CO_3 . Conversion from **3** to **10** was achieved in an overall yield of 61%. The deprotected alcohol (**11**) was converted to **6** by treatment with

(14) Sundararajan, C.; Falvey, D. E. *Photochem. Photobiol. Sci.* **2006**, *5*, 116–121. (a) Kottani, R.; Valiulin, R. A.; Kutateladze, A. G. *PNAS* **2006**, *103* (38), 13917–13921.

(15) Blake, J. A.; Gagnon, E.; Lukeman, M.; Scaiano, J. C. *Org. Lett.* **2006**, *8* (6), 1057–1060.

(16) Rewcastle, G. W.; Atwell, G. J.; Baguley, B. C.; Calveley, S. B.; Denny, W. A. *J. Med. Chem.* **1989**, *32* (4), 793–799.

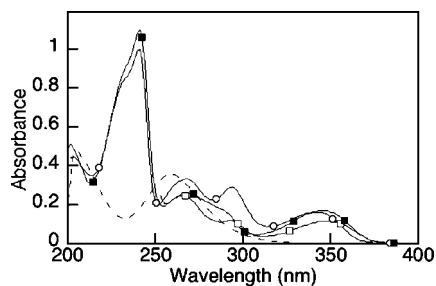


Figure 1. Absorption spectra of **1** (---), **3** (□), **4** (○), **5** (■) 2×10^{-5} M in pH 7.4 phosphate buffer.

acetic anhydride. Synthesis of **12** was achieved by the treatment of aniline with $1/3$ equiv of triphosgene with triethylamine, followed by the addition of 1 equiv of **10**. Deprotection yielded the final product, **7**. Since the photolabile protecting group is based on xanthone propionic acid, we abbreviate this PPG as XPA.

Photochemistry of 3–5. The photochemistry of **3–5** was investigated in aqueous solution to ascertain whether they are capable of undergoing photodecarboxylation to give carbanion intermediates that are necessary for the eventual photorelease mechanism of **6** and **7**. Irradiation of a 8 mM sample of **3** in buffered aqueous solution (Luzchem LZC-ORG photoreactor, 10 UVA lamps, pH 7.4, nitrogen bubbled) for 3 min resulted in its clean transformation to 2-methylxanthone (**13**) in 27% yield (Scheme 3). This reaction was conveniently followed by ^1H NMR, with irradiation leading to the growth of a characteristic singlet at 2.5 ppm that is assigned to **13**, at the expense of the singlet at 3.8 ppm that is assigned to the methylene protons of the starting material. Extensive irradiation (30 min) of **3** resulted in complete conversion to **13**, with no other products observed by ^1H NMR, HPLC-UV, or GC-MS analysis. Remarkably, this photochemistry was equally clean in aerated and deaerated solutions. Irradiation of **5** under the same conditions gave 4-methylxanthone (**14**) as the only observable product (Scheme 4). Exclusive photogeneration of **13** and **14** on irradiation of **3** and **5**, respectively, is consistent with a heterolytic mechanism in which only carbanion intermediates are formed. In addition, since ketoprofen photodecarboxylation under air leads to two minor photoproducts that are attributed

Scheme 4. Photodecarboxylation of 2- and 4-Xanthone Acetic Acid (**3** and **5**)

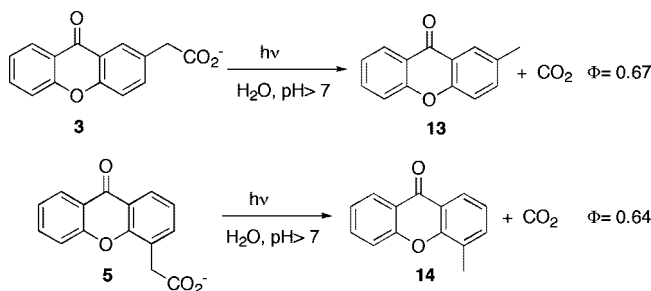


Table 1. Photophysical Parameters for 2-, 3-, and 4-Xanthone Acetic Acid (**3–5**) and 2- and 4-Methylxanthone (**13, 14**)

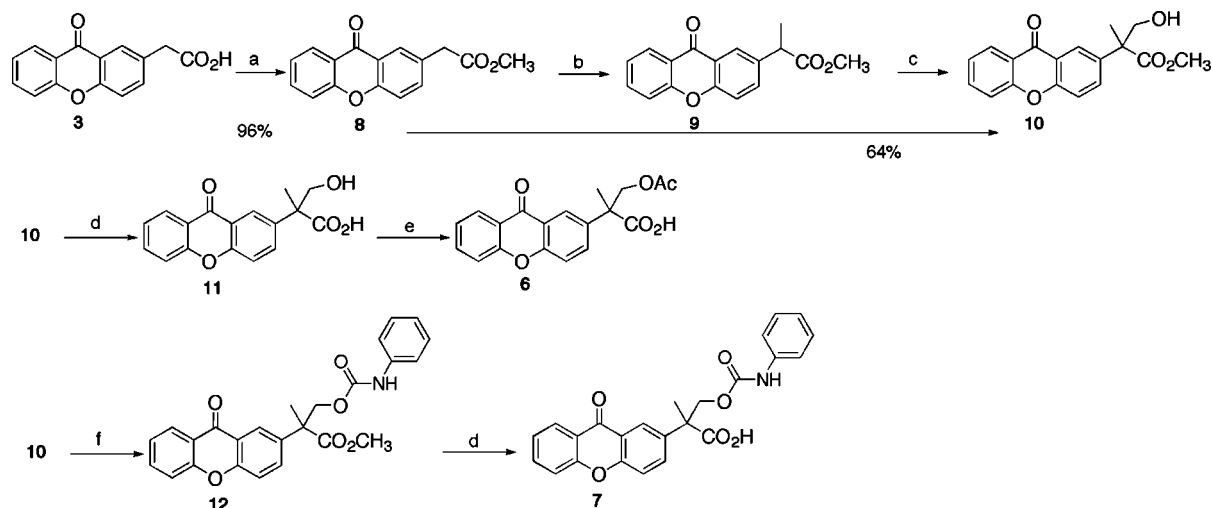
compound	$\Phi_{\text{F}}^{\text{a}}$	$\Phi_{\text{F}}^{\text{b}}$	τ_{S} (ns) ^c	k_{F} (ns ⁻¹) ^d	τ_{T} (ns) ^e	triplet yields
3	0.67	0.0077	0.079	0.098	5400	0.4
4	<0.01	0.044	0.73	0.061	4500	1.1
5	0.64	0.010	0.10	0.097	6600	0.3
13	–	0.24	4.8	0.051	9500	1.0
14	–	0.15	3.9	0.039	6200	(1.0) ^f

^a pH 7.4 phosphate buffer using ketoprofen as a reference. ^b pH 7.4 phosphate buffer using quinone bisulfate as a reference. ^c pH 7.4 phosphate buffer with 20% acetonitrile by fluorescence emission with 30 ps excitation at 355 nm, streak camera detection. ^d Calculated from Φ_{F} and τ_{S} . ^e pH 7.4 phosphate buffer with 20% acetonitrile by ns LFP using 355 nm excitation. ^f Used as a reference for relative triplet yields.

to reaction of the carbanion with oxygen,¹⁰ the absence of equivalent photoproducts from xanthone acetic acid in aerated solutions suggests a very short lifetime of the xanthone acetic acid carbanion (<20 ns) consistent with laser flash photolysis experiments where we were unable to observe the carbanion intermediate (*vide infra*).

Reaction quantum yields for the decarboxylation of **3** and **5** were measured using the analogous reaction of ketoprofen as a secondary reference standard ($\Phi = 0.75$ at pH 7.4) and appear in Table 1. Both isomers show a photodecarboxylation efficiency that is close to that of ketoprofen, demonstrating that the addition of the bridging oxygen does not significantly perturb the photochemistry.¹⁷

Scheme 3^a



^a Reaction conditions: (a) 5% $\text{H}_2\text{SO}_4/\text{MeOH}/\text{reflux}$; (b) (i) LDA/THF , (ii) CH_3I ; (c) $(\text{CH}_2)_n/\text{K}_2\text{CO}_3/\text{DMSO}$; (d) $\text{CH}_3\text{CN}/0.1 \text{ M KOH}$; (e) acetic anhydride; (f) triphosgene/aniline/ $\text{Et}_3\text{N}/\text{CH}_2\text{Cl}_2$.

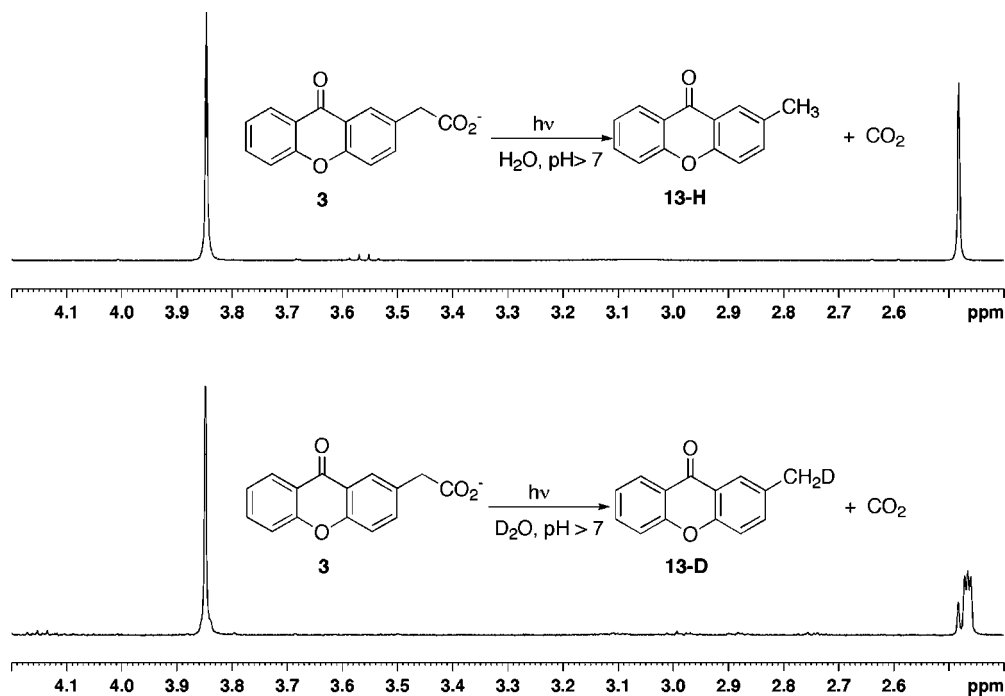


Figure 2. ^1H NMR spectra of **3** (8 mM) irradiated in H_2O with 0.1 M KOH (top) and **3** irradiated in D_2O with 0.1 M KOH (bottom). Samples were irradiated simultaneously with UVA light. The bottom spectrum shows formation of **13-H** (singlet) in addition to **13-D** (triplet), presumably due to the presence of residual H_2O .

To our surprise, irradiation of **4** did not give any decarboxylation products, and even on extended photolysis, the complete recovery of starting material was realized. Such a stark contrast in photodecarboxylation reactivity between positional isomers is rare; for the related 3- and 4-benzoylphenylacetic acids,¹⁸ and for 3- and 4-nitrophenyl acetic acids,¹⁹ the difference in photodecarboxylation efficiency between isomers is very small. We believe that the lower reactivity of **4** is a consequence of the “*meta* effect”, which is the prediction from MO theory that, in the excited state, activating groups on aromatic rings will have a stronger influence on the reaction center when they are positioned *meta* to it rather than *para*, which is the reverse of the ground-state ordering.²⁰ The activating group in these examples is the carbonyl group which is *meta* to the acetic acid group in reactive isomers **3** and **5** but is *para* in the nonreactive isomer **4**. In addition, there may be a *meta* deactivating effect from the aryl ether group.

To provide additional evidence of the intermediacy of carbanion intermediates in the photodecarboxylation of **3** and **5**, solutions of **3** and **5** were irradiated in H_2O and D_2O (each containing 0.1 M KOH), and the photolysates were analyzed by ^1H NMR. Irradiation of **3** or **5** in D_2O solution gave the corresponding α -deuteromethylxanthone (**13-D** or **14-D**) with a small amount of **13-H** or **14-H**, presumably due to the presence of residual H_2O , as the only products observable by ^1H NMR. The α -deuteromethylxanthenes were easily recognizable by ^1H NMR, since the CH_2D signal exhibits the characteristic triplet and is slightly upfield from the CH_3 signal from the corresponding methylxanthone (Figure 2) and integrates for two hydrogens relative to the aromatic signals of **13-D** or **14-D** (see Supporting Information). Since D_2O is a very poor deuterium atom donor, but an excellent D^+ source, these results support the intermediacy of a carbanion rather than a radical.

Photochemistry of 6–7. Having established that **3** and **5** are efficient photochemical sources of carbanion intermediates, we

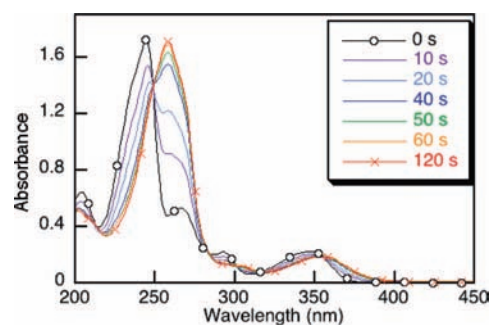
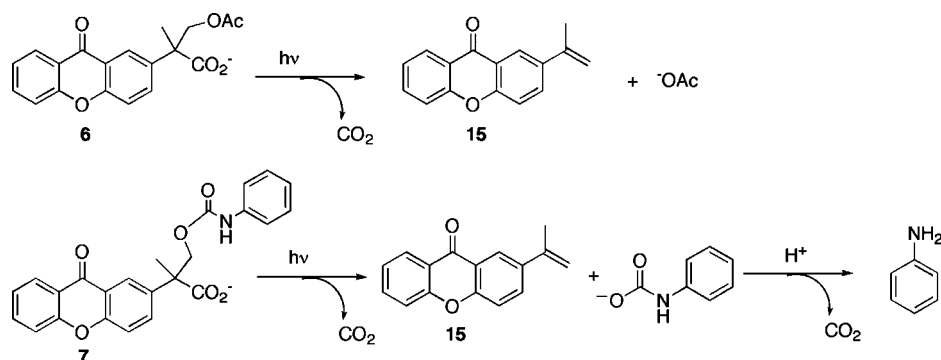


Figure 3. UV–vis traces of **6** in 4.0×10^{-5} M solution after times indicated in the legend.

then sought to harness this reactivity to effect the photorelease of anionic leaving groups. We decided to design our PPGs **6** and **7** based on the structure of **3** because of its slightly higher quantum yield relative to **5** (Table 1), although we expect that PPGs based on **5** would likely show similar chemistry. Irradiation of **6** in a 10 mm quartz cuvette (2 UVA lamps, 4.0×10^{-5} M in pH 7.4 phosphate buffer solution) led to significant changes in the absorption spectra with peaks characteristic of the starting material decreasing concomitant with new peaks emerging at 258, 305, and 354 nm (Figure 3). Sharp isosbestic points were observed at 248, 284, 300, 316, and 355 nm, suggesting that irradiation of **6** gives only a single photostable product that absorbs in this region. Such changes are consistent with a clean photochemical reaction that significantly perturbs the chromophore, as might be expected from the exclusive photogeneration of alkene **15** via the anticipated elimination pathway (Scheme 5 top). Interestingly, the chromophore is bleached by a factor of 1.5 at the wavelength of a nitrogen laser (337 nm). At other wavelengths however, this is not the case so linear conversion is limited to low concentrations ($<10^{-3}$ M). To better characterize the reaction photoproduct, irradiations of preparative scale solutions of **6** were carried out. Following organic

Scheme 5. Photorelease of Acetate (Top) and Aniline via Its Carbamate (Bottom)

extraction from the acidified photolysate, the isolated white solid was analyzed by ^1H NMR. Irradiation of **6** (4 UVB lamps, 1.0×10^{-3} M in pH 7.4 phosphate buffer solution) for 15 min resulted in the complete loss of the methylene and acetate ^1H NMR signals attributed to **6**. New peaks were observed at 5.24 and 5.59 ppm which correspond to the alkene protons of expected photoproduct **15**. HPLC-UV and GC-MS confirmed the complete conversion of **6** to **15** after 15 min of irradiation with no other photoproducts detected, confirming that the photoreaction proceeds cleanly and that **15** is photostable under these conditions. Quantitative formation of **15** implies that we have achieved quantitative release of a carboxylic acid in this reaction.

Compound **7** was designed to release aniline by first releasing its carbamate which will subsequently decarboxylate thermally to give the aromatic amine²¹ (Scheme 5 bottom). Irradiation of **7** was conducted under similar conditions as described above for **6**. ^1H NMR analysis of the photolysate from a solution of **7** revealed singlets at 5.24 and 5.59 ppm corresponding to alkene **15** as the only new peaks, indicating that we have achieved quantitative release of the aniline from **7** via its carbamate.

Fluorescence. The mechanism of photodecarboxylation from ketoprofen (**1**) has been a source of interest for almost two decades, with the multiplicity of the reactive state being a primary issue. It is well-known that aromatic ketones will typically react via their triplet excited states, in fact a number of PPGs depends on such chemistry.²² However, evidence in favor of a singlet decarboxylation mechanism for ketoprofen has been presented.¹¹ One difficulty in unequivocally determining the multiplicity of the reactive state arises from the fact that ketoprofen is not fluorescent in solution, thus depriving us of a very useful tool in studying singlet excited states. Xanthone and its derivatives are weakly fluorescent in solution, and the dependence of the fluorescence of xanthone on the nature of the solvent has been well studied.²³ Thus we employed fluorescence experiments to aid in the elucidation of the mechanism of decarboxylation of the xanthone acetic acids studied.

Xanthone acetic acids **3–5** showed weak fluorescence emission with λ_{max} at 410, 390, and 405 nm, respectively, in neutral phosphate buffer solution (absorbance = 0.1 or 0.05 at λ_{ex}). Photoproducts **13** and **14** have dramatically larger fluorescence quantum yields relative to their parent acids (Table 1). As such, the fluorescence signal from aqueous solutions of **3** or **5** can be observed to increase rapidly with irradiation (data for **3** shown in Figure 4). Solutions of **3** experience a 30-fold enhancement in fluorescence emission following 60 s of exposure to the UVA output of a hand-held TLC lamp ($\lambda_{\text{max}} = 368$ nm, fwhm = 16 nm). Solutions of **5** experience a 15-fold enhancement.

We have measured the fluorescence lifetimes for reactive xanthone derivatives **3** and **5** as well as photostable **4**, **13**, and **14** (Figure 5, Table 1). Using the measured fluorescence quantum yields (Φ_{F}) and singlet state lifetimes (τ_{S}), a fluorescence rate constant (k_{F}) can be calculated for **3–8** since $\Phi_{\text{F}} = k_{\text{F}}/k_{\text{S}} = k_{\text{F}}\tau_{\text{S}}$. Since k_{F} is calculated to be roughly the same for each of our xanthone derivatives, but the reactive **3** and **5** have much shorter singlet state lifetimes, there must be an additional process occurring from the singlet excited states of **3** and **5**. We attribute this process to singlet state photodecarboxylation.

The observed fluorescence increase may also serve as a valuable "reporting" tool since fluorescence increases dramatically with photorelease, thus having the potential to be used as a mapping tool in biological systems.

Nanosecond Laser Flash Photolysis (LFP). In the hope of observing the carbanion intermediates produced on photodecarboxylation of **3** and **5**, we employed nanosecond laser flash

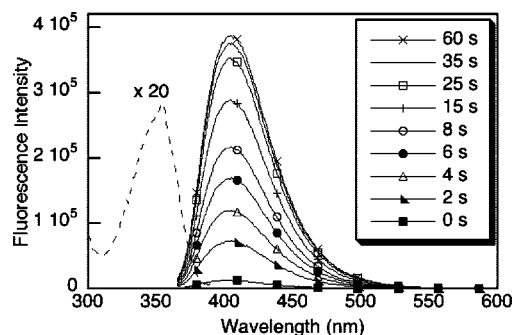


Figure 4. Fluorescence increase as a solution of **3** is irradiated (solid lines). Excitation spectrum of **3** magnified by a factor of 20 (dashed line).

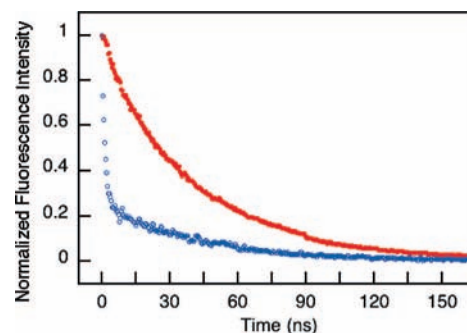


Figure 5. Decay of fluorescence from **5** (blue) and **14** (red). The blue trace decays with two components. The shorter of these two is assigned to **5** while the longer component corresponds to the fluorescence decay of a small amount of **14**. Time constants were obtained by fitting the trace after deconvoluting the laser pulse.

photolysis (LFP). The transient spectra of **3**, **4**, and **5** contained broad absorption bands centered at 580, 600, and 585 nm, respectively, that in all cases decayed with clean first-order kinetics. The transients produced from **3–5** upon 355 nm excitation showed similar lifetimes of $\sim 5 \mu\text{s}$ (table 1) in N_2 saturated solutions. These transient absorption spectra are similar in λ_{max} , spectral width, and lifetime to the triplet of the parent xanthone.²⁴ When solutions were saturated with oxygen, similar transient absorption spectra were obtained, although the transient lifetime was reduced to 0.4, 0.2, and 0.3 μs for **3**, **4**, and **5**, respectively. Since oxygen is well-known to be an effective quencher of triplet states, we propose that the long-lived signals we see from **3–5** are due to triplet–triplet absorptions.

To confirm this assignment, we employed other triplet quenchers including 1-hydroxymethylnaphthalene (HMN) and potassium sorbate. Addition of HMN to solutions of **3–5** led to an increase in the decay rate constant for their respective triplet signals, along with a growth at $\sim 420 \text{ nm}$, which is characteristic of the triplet signal of the naphthalene chromophore.²⁵ This result is strong support for our assignment of the transients from **3–5** as triplet states, since quenching of triplets by HMN will produce a naphthalene triplet signal. Because the naphthalene triplet at 420 nm appears as a growth, we can be confident that the signal is not due to direct excitation of HMN (which in any case does not absorb at the excitation wavelength of 355 nm). Addition of increasing amounts of HMN allowed us to produce a quenching plot, whose slope gave a bimolecular quenching rate constant of $4.4 \times 10^9 \text{ M}^{-1} \text{ s}^{-1}$.

We also used potassium sorbate to quench the triplets we observed on LFP of **3–5**. Efficient quenching was observed on addition of the sorbate, and by varying the sorbate concentration, we were able to produce the quenching plot shown in Figure 6. The quenching plot showed a linear correlation, and the slope indicated a bimolecular quenching rate constant of $2.7 \times 10^9 \text{ M}^{-1} \text{ s}^{-1}$. Due to the high solubility of potassium sorbate in water, we were able to use sufficiently large concentrations to quench the triplet signal from **3–5** entirely. We were hoping that, by completely quenching the triplet, we might detect a possible carbanion signal that had previously been obscured by the much larger triplet signal. On addition of 50 mM potassium

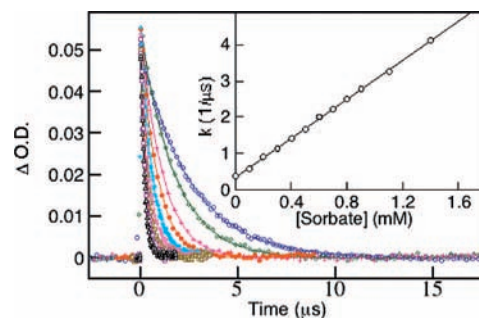
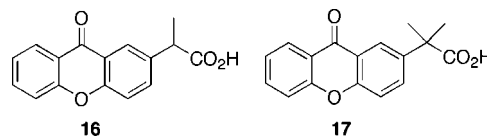


Figure 6. Quenching by sorbate of transient decays for 0.08 mM **4** in deaerated pH 7.4 phosphate buffer/acetonitrile. Inset: rate constant of each decay as a function of sorbate concentration.

sorbate, we were unable to detect any transient absorption by LFP, suggesting that the carbanion lifetime is too short for us to detect within the time resolution of our instrument ($\sim 20 \text{ ns}$). With the knowledge that addition of 50 mM potassium sorbate to solutions of **3–5** leads to $>95\%$ quenching of the photogenerated triplet states, we repeated the product studies with potassium sorbate to see if quenching the triplets would affect product yields. Solutions of **3** in pH 7.4 phosphate buffer with and without 50 mM sorbate were irradiated simultaneously in a carousel, and the photoproducts were analyzed. We found that the presence of sorbate had no effect whatsoever on product yields. This is strong evidence that the photodecarboxylation of **3** occurs *exclusively* from the singlet excited state and that the triplet state does not play a measurable role in the photodecarboxylation mechanism and, by extension, the photorelease mechanism. This is very unusual behavior for aromatic ketones whose photochemistry is frequently dominated by triplet processes.

We attempted to increase the lifetime of the carbanion produced on photodecarboxylation of **3** so that we could characterize it by LFP. We decided to substitute the benzylic carbon of **3** with alkyl groups, a strategy that we have previously shown to be successful in prolonging the lifetimes of similar carbanions from ketoprofen due to steric shielding by the alkyl groups.¹³ To this end, we prepared mono- and dimethylated derivatives **16** and **17**, although LFP of these analogues in 0.1 M KOH or D_2O with NaH, both with 50 mM sorbate to remove the triplet signal, failed to produce a detectable signal. It would seem that the carbanion intermediates from **3** and **5** are very short-lived and that the lifetime enhancement provided by the benzylic alkyl groups was too modest to enable us to detect their absorption.



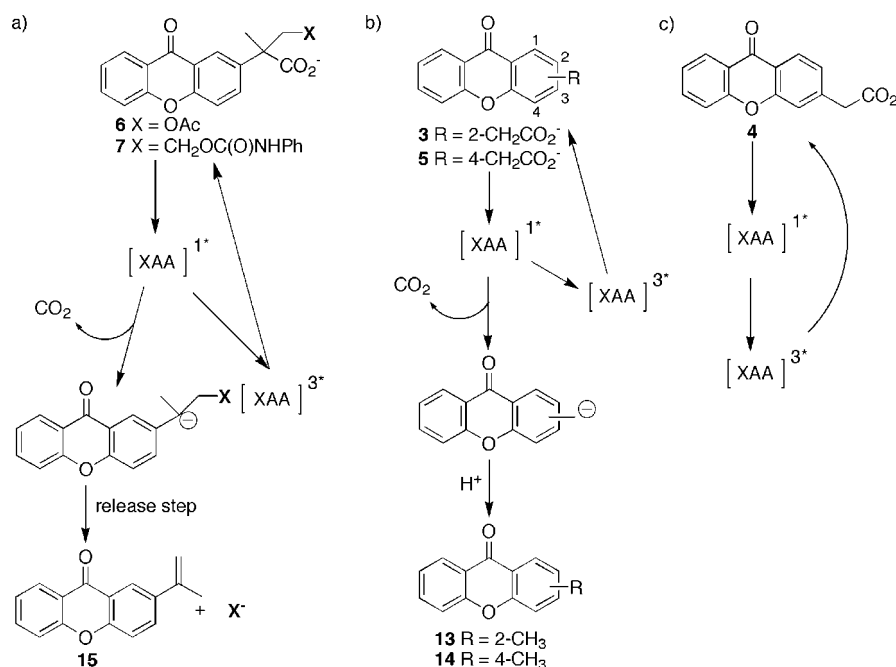
Mechanism of Photodecarboxylation and Photorelease. Irradiation of **3** and **5** in aqueous and deuterated aqueous solutions gave products consistent with exclusive formation of a carbanion intermediate via photodecarboxylation, and the fluorescence and quenching experiments support a singlet pathway. We were able to directly detect strong triplet signals for **3–5** via LFP, indicating that intersystem crossing is significant. Our quenching studies with sorbate allow us to rule out triplet state photodecarboxylation, proving that this proceeds exclusively from the singlet state. Our inability to detect carbanion signals via LFP

- (17) We note that we have also detected photodecarboxylation of **3** and **5** under acid conditions, where the carboxylic acid moiety will not be extensively ionized, at least in the ground state. This observation is still under study; the current contribution centers on the behavior of the carboxylate form under biologically relevant conditions.
- (18) Xu, M.; Wan, P. *Chem. Commun.* **2000**, 2147–2148.
- (19) Margerum, J. D.; Petrusis, C. T. *J. Am. Chem. Soc.* **1969**, *91* (10), 2467–2472.
- (20) Zimmerman, H. E. *J. Am. Chem. Soc.* **1995**, *117* (35), 8988–8991.
- (21) Papageorgiou, G.; Barth, A.; Corrie, J. E. T. *Photochem. Photobiol. Sci.* **2005**, *4*, 216–220.
- (22) Klán, P.; Zabadal, M.; Heger, D. *Org. Lett.* **2000**, *2*, 1569–1571. (a) Klán, P.; Pelliccioli, A. P.; Pospisil, T.; Wirz, J. *Photochem. Photobiol. Sci.* **2002**, *1*, 920–923. (b) Literák, J.; Wirz, J.; Klán, P. *Photochem. Photobiol. Sci.* **2005**, *4*, 43–46. (c) Pika, J.; Konosonoks, A.; Robinson, R. M.; Singh, P. N. D.; Gudmundsdóttir, A. D. *J. Org. Chem.* **2003**, *68* (5), 1964–1972.
- (23) Abdullah, K. A.; Kemp, T. J. *J. Photochem.* **1986**, *32*, 49–57. (a) Scaiano, J. C.; Weldon, D.; Pliva, C. N.; Martínez, L. J. *J. Phys. Chem. A* **1998**, *102*, 6898–6903. (b) Heinz, B.; Schmidt, B.; Root, C.; Satzger, H.; Milota, F.; Fierz, B.; Kiefhaber, T.; Zinth, W.; Gilch, P. *Phys. Chem. Chem. Phys.* **2006**, *8* (29), 3432–3439.
- (24) Scaiano, J. C. *J. Am. Chem. Soc.* **1980**, *102*, 7747. (a) Evans, C. H.; Prud'homme, N.; King, M.; Scaiano, J. C. *J. Photochem. Photobiol. A: Chem.* **1999**, *121*, 105–110.
- (25) Grabner, G.; Rechthaler, K.; Mayer, B.; Köhler, G. *J. Phys. Chem. A* **2000**, *104*, 1365–1376. (a) Bensasson, R.; Land, E. *J. Trans. Faraday Soc.* **1971**, *67*, 1904–1915.

Table 2. Comparison of the Properties of *o*-NB, Ketoprofenate, and Xanthone PPG for Carboxylate Release

PPG	Φ_{release}	λ_{max} , nm (ϵ , M ⁻¹ cm ⁻¹)	τ_{release}	suitable conditions and solubility	fluorescence reporting
<i>o</i> -NB or close derivative	<0.2 ^a depending on the <i>o</i> -NB substituents	262 (5100) ^{a,b}	microsecond ^a	solubility depends on the <i>o</i> -NB substituents	not reported
ketoprofenate	>0.7	259 (18 000)	sub-nanosecond	limited to physiological conditions (aqueous, pH > 6)	PPG and photoproduct are both nonfluorescent
xanthone	>0.6	348 (5600)	sub-nanosecond	limited to physiological conditions (aqueous, pH > 6)	fluorescence increase ($\times 30$) can be used to report release

^a Summarized in ref 1, Chapter 1. ^b Based on α -carboxy-2-nitrobenzyl protected glutamate.

Scheme 6. Photorelease Mechanism from **6** and **7** (a) and Summary of the Photophysical and Photochemical Processes for Xanthone Acetic Acids (XAA) **3** and **5** (b) and **4** (c)

of **3**, **5**, and alkyl derivatives of **3** (**16** and **17**) and our inability to trap the intermediate carbanions with oxygen indicate that the carbanions produced are very reactive, much more so than the carbanion derived from ketoprofen.

Initially it was not clear to us whether or not a more reactive carbanion would be beneficial for the photoelimination of leaving groups. On one hand, a rapid trapping of the carbanions by water would provide a formidable competing pathway for the desired elimination. On the other hand, increasing the reactivity of the carbanion should accelerate unimolecular reactions (i.e., elimination) at the expense of bimolecular reactions (i.e., protonation). As we have observed only the elimination product **15** on irradiation of **6** and **7**, it would appear that increasing the reactivity of the carbanion is not deleterious for the elimination of good leaving groups such as carboxylates and carbamates. Since the carbanion intermediates produced on irradiation of **3**, **16**, and **17** were all too short-lived for us to observe by LFP, we can estimate an upper limit of 20 ns for their lifetimes, which gives us pseudo-first-order protonation rate constants of $\geq 5 \times 10^7$ s⁻¹. Since we only see elimination photoproducts from **6** and **7**, we can assume that >95% of the carbanions generated follow the elimination pathway, indicating that the elimination rate constant is at least 20 times that of the protonation rate constant. These assumptions allow us to

estimate a *minimum* elimination rate constant of 10⁹ s⁻¹, which means that the elimination of leaving groups from **6** and **7** occurs in less than 1 ns. This represents an improvement in photorelease rates of ~ 5 orders of magnitude when compared with the *o*-NB system! It should be noted at this point that the leaving group from **7** refers to the intermediate ⁻OC(O)NHC₆H₅ rather than aniline itself. The actual release of aniline is rate limited by the dark decarboxylation step,²¹ a common drawback associated with the release of amines. The photoprocesses described above are summarized in Scheme 6.

Conclusion

In a recent publication (Chapter 1 in ref 1), Corrie identified the difficulty in predicting reaction rates or efficiencies as a current challenge in the field of photolabile protecting groups. This difficulty often arises from a lack of information regarding the release mechanism. In fully characterizing the photochemical mechanism of release for this new xanthone PPG, we hope to demonstrate a more predictable release. In particular, we are confident that the "xanthone" PPG photorelease of acetate and aniline (via the carbamate) can be extended to other carboxylic acids and amines (via the carbamates) since the key steps of the release mechanism do not involve the substrate and the release occurs so rapidly that interference from the substrate is

not likely except in special cases where energy or electron transfer with the substrate is possible.

Xanthone based photocages have been shown to have major advantages over *o*-NB and ketoprofenate cages, combining the high quantum yields and chemical yields of the system with good UVA absorption properties, ultrafast release, and the formation of fluorescent photoproducts that may find use as reporters in the mapping of release sites in biological systems.

Experimental Section

All starting materials used in this work were purchased from Sigma-Aldrich Canada (Oakville, ON) and used without further purification. Solvents were dried by the usual methods. DMSO was purchased as an anhydrous grade and stored over molecular sieves. Column chromatography employed Merck silica gel 230–400 mesh. ^1H and ^{13}C NMR spectra were recorded at room temperature at 400 MHz. Chemical shifts are reported relative to internal TMS.

Synthesis. The synthesis and characterization of **3–5**, **13**, and **14** were previously reported.¹⁵

Methyl-2-(9-oxo-9H-xanthen-2-yl)propanoate (9). A stirred solution of **8** (1.07 g, 3.99 mmol) in dry THF was cooled in a dry ice/acetone bath ($-78\text{ }^\circ\text{C}$) under a nitrogen atmosphere. To this was added LDA freshly prepared from diisopropylamine and standardized *n*-BuLi (2.5 M, 4.39 mmol). After 30 min, once the blue color of the carbanion had evolved, iodomethane (5.99 mmol) was added. The solution was allowed to warm gradually to room temperature. The reaction was quenched with water and transferred to a separatory funnel with ethyl acetate for extraction. Organic layers were washed with NaHCO_3 , dried over MgSO_4 , and concentrated under vacuum. Recrystallization from hot ethanol yielded **9** as a white solid with 16% of the dimethylated product (**17**) as determined by ^1H NMR.

Methyl 3-Hydroxy-2-methyl-2-(9-oxo-9H-xanthen-2-yl) (10). To a solution of nitrogen purged DMSO with paraformaldehyde and K_2CO_3 (both partially dissolved) **9** (with 16% **17**) was added. The solution was stirred at room temperature overnight under a positive pressure of nitrogen. After filtering, the reaction was quenched with 1% HCl and extracted with CH_2Cl_2 . The combined organic layers were washed with 1% HCl, dried (MgSO_4), and concentrated in vacuo to give an oil that was further purified by flash chromatography (100 g silica, 30% ethyl acetate in hexanes). Yield from **8** = 64% (2.56 mmol). ^1H NMR (400 MHz, CDCl_3) δ 8.30 (dd, 1H, $J = 1.6$ Hz), 8.25 (d, 1H, $J = 2.4$ Hz), 7.73–7.66 (m, 2H), 7.44 (t, 2H, $J = 8.8$ Hz), 7.36 (t, 2H, $J = 7.4$ Hz), 4.10 (d, $J = 11.2$ Hz, 1H, $-\text{CH}_2-$), 3.82 (d, $J = 11.2$ Hz, 1H, $-\text{CH}_2-$), 3.74 (s, 3H, $-\text{CH}_3$), 2.98 (s broad, 1H, $-\text{OH}$), 1.76 (s, 3H, $-\text{CH}_3$). ^{13}C NMR (100 MHz, CDCl_3) δ 176.9 (CO), 176.0 (CO), 156.0, 155.2, 136.6 (quaternary aromatic), 134.9, 133.5, 126.7, 124.1, 124.0 (CH aromatic), 121.6, 121.4 (quaternary aromatic), 118.3, 117.9 (CH aromatic), 69.4 (CH_2), 52.5 (CH_3), 52.3 (quaternary), 20.4 (CH_3).

3-Acetoxy-2-methyl-2-(9-oxo-9H-xanthen-2-yl)propanoic acid (2-XPA-OAc) (6). To a 100 mL round-bottom flask **11** (0.46 mmol) was added with 50 mL of CH_2Cl_2 , 0.3 mL of pyridine, and 0.6 mL of acetic anhydride. The mixture was stirred for 3 h at room temperature, transferred to a separatory funnel, washed with 1% HCl (50 mL), and then concentrated under vacuum. The residue was dissolved in 100 mL of a 1:1 $\text{CH}_3\text{CN}-\text{H}_2\text{O}$ mixture and stirred overnight at room temperature to decompose any remaining anhydride. The mixture was diluted with 50 mL of CH_2Cl_2 and then washed with 50 mL of 1% HCl. The organic layer was dried with MgSO_4 , and the solvent was removed under vacuum to yield a white solid (0.33 mmol, 72%). ^1H NMR (400 MHz, acetone- d_6) δ 8.31 (d, 1H, $J = 2.4$ Hz), 8.26 (dd, 1H, $J = 1.6$ Hz, 8 Hz), 7.8–8.0 (m, 2H), 7.62 (t, 2H, $J = 8.8$ Hz), 7.47 (t, 1H, $J = 7.6$ Hz), 4.60 (d, 1H, $J = 10.8$ Hz), 4.50 (d, 1H, $J = 10.8$ Hz), 1.98 (s, 3H), 1.77 (s, 3H). ^{13}C NMR (100 MHz, acetone- d_6) δ 205.3 (aromatic CO), 175.5, 169.7 (CO), 156.0, 155.3, 136.7 (aromatic

quaternary), 135.2, 133.6, 126.2, 124.2, 123.8 (aromatic CH), 121.6, 121.3 (aromatic quaternary), 118.4, 118.1 (aromatic CH), 68.7 ($-\text{CH}_2-$), 49.5 (quaternary), 20.34 ($-\text{CH}_3$), 19.77 ($-\text{CH}_3$). HRMS calcd 340.0947, found 340.0939.

Methyl 2-Methyl-2-(9-oxo-9H-xanthen-2-yl)-3-(phenylcarbamoyloxy)propanoate (12). Triphosgene (0.49 mmol, 0.145 g) was dissolved in 3 mL of CH_2Cl_2 . Aniline and triethylamine were dissolved in 7 mL of CH_2Cl_2 and then added dropwise over 1 h to triphosgene at room temperature. To this was added **10** (0.23 g, 0.74 mmol) dissolved in 2 mL of CH_2Cl_2 . The solution was stirred under nitrogen for 15 h and then quenched with water. The solvent was removed under vacuum, and the reaction was extracted with EtOAc. Combined organics were washed with saturated NaHCO_3 and then brine and dried with MgSO_4 . The solvent was removed under vacuum to yield an oil. Pure **12** was isolated by column chromatography. ^1H NMR (400 MHz, CDCl_3) δ 8.3 (two ds, 2H, $J = 2.4$ Hz, 1.6 Hz), 7.73 (m, 2H), 7.47 (t, 2H, $J = 8.8$ Hz), 7.38 (m with broadening possibly due to rotational hindrance, 5H), 7.03 (t, 1H, $J = 8.4$ Hz), 6.95 (s broad, NH), 4.71 (d, 1H, $J = 10.8$ Hz), 4.60 (d, 1H, $J = 10.8$ Hz), 3.73 (s, 3H), 1.77 (s, 3H). ^{13}C NMR (100 MHz, CDCl_3) δ 176.9, 174.0 (CO), 156.1, 155.4, 137.7, 135.9 (aromatic quaternary), 135.0, 133.2, 129.0, 126.8, 124.3, 124.1, 123.5 (aromatic CH), 121.7, 121.5 (aromatic quaternary), 118.5, 118.0 (aromatic CH), 69.4 (CH_2), 52.7 (CH_3), 50.5 (quaternary), 20.9 (CH_3). Deprotection of the methyl ester yielded **7**.

2-Methyl-2-(9-oxo-9H-xanthen-2-yl)propanoic Acid (17). 8 (0.11 g, 0.41 mmol) was dissolved in 10 mL DMSO. After purging with nitrogen gas, crushed KOH (0.2 g) was added. Once the blue color of the carbanion evolved, excess CH_3I was added and the solution was stirred under nitrogen gas for 3 h. The reaction was quenched with 1% HCl and extracted with CH_2Cl_2 . The combined organic layers were washed thoroughly with 1% HCl, dried (MgSO_4), and concentrated in vacuo to give an oil that was further purified by flash chromatography (100 g silica, 25% ethyl acetate in hexanes). The methyl ester was deprotected using the same method as that for **11**, and **17** was obtained as a white solid. ^1H NMR (400 MHz, CDCl_3) δ 8.35 (2H), 7.71 (2H), 7.47 (2H), 7.38 (1H), 3.68 (3H), 1.68 (6H).

Product Studies. For initial photolysis product studies, an 8 mM solution of one of **3–5** in either 0.1 M KOH or 0.1 M phosphate buffer adjusted to pH 7.4 was irradiated in a Luzchem ORG photoreactor equipped with eight UVA lamps (~ 350 nm). Following irradiation, the contents of each tube were acidified with 1 M HCl and extracted with CH_2Cl_2 . The recovered white solid from each was dissolved in DMSO- d_6 or acetone- d_6 and analyzed by ^1H and ^{13}C NMR.

Nanosecond Laser Flash Photolysis. The laser flash photolysis system is a customized system operated with Luzchem software. Kinetics and spectra were obtained by exciting with the third harmonic of a Surelite Nd:YAG laser generating pulses at 355 nm of an 8 ns duration and a 20 mJ output. Spectra and kinetic experiments of **4** employed 7×7 mm² quartz cells with a static solution, while experiments with **3** and **5** employed 7×7 mm² quartz flow cells with solutions flowed at a high rate with constant bubbling of either nitrogen or oxygen as specified. Lifetimes of the triplet signal for **3–5** were measured for both solutions with $A = 0.15$ and $A = 0.30$. Spectra and quenching studies were measured for solutions with $A = 0.30$.

Fluorescence Spectroscopy. All solutions under study were thoroughly deaerated with dry nitrogen prior to fluorescence measurements. Steady-state fluorescence spectra were collected with a luminescence spectrometer from Photon Technology International. Time-resolved studies were made with the third harmonic of a Continuum PY-61 Nd:YAG laser ($\lambda_{\text{ex}} = 355$ nm, fwhm = 35 ps, pulse energy = 4 mJ), using a Hamamatsu C4334 streak camera for luminescence detection.

Acknowledgment. J.C.S. and M.L. acknowledge the generous financial support of the Natural Sciences and Engineering Research

Council (NSERC). J.C.S. thanks the Canadian Institutes of Health Research (CIHR), the Canadian Foundation for Innovation and the province of Ontario. J.A.B. thanks NSERC for a postgraduate scholarship. We acknowledge Professor May Griffith for stimulating our interest in medical applications of xanthone photocages.

Supporting Information Available: Chart of structures; absorption coefficients; description of photolysis experiments

with full ^1H NMR for **3** irradiated in basic H_2O and D_2O ; description of fluorescence measurements; modeling of the singlet excited state and ground state of xanthone; LFP spectra; ^1H NMR of **6** and **7** demonstrating release and ^1H NMR of **12**. This material is available free of charge via the Internet at <http://pubs.acs.org>.

JA8094872